corrections were applied from ϕ scans of four reflections.

The structures were solved using the heavy-atom method. After refinement of the heavy atoms, a difference-Fourier map revealed maxima of residual electron density close to the positions expected for hydrogen atoms; they were introduced in calculations in calculated positions (C–H = 0.95 Å) with isotopic temperature factors such as $B(H) = 1.3B_{eqv}(C)$ Å^2 but were not refined. Full least-squares refinements were done; $\sigma^2(F^2) = \sigma^2_{counts} + (pI)^2$. The absolute structure of compound **6** was determined by comparing x,y,z and $-x,-y,-z$ refinements. A final difference map revealed no significant maxima. The scattering factor coefficients and anomalous dispersion coefficients come from ref 20.

Acknowledgment. Financial support from the MRT (Ministère de la Recherche et de la Technologie) (to J.P.S.) is gratefully acknowledged; we thank Prof. Rheingold for providing us the X-ray data of compound **2**.

Registry No. **1**, 58616-62-9; **2**, 137429-17-5; **3**, 137429-18-6; **4**, 137259-11-1; **5**, 137259-12-2; **6**, 137300-26-6; **7**, 137429-19-7; 3-hexyne, 928-49-4; maleic anhydride, 108-31-6.

Supplementary Material Available: Tables of positional parameters of the hydrogen atoms (Tables SI, SVI, SXI), bond distances (Tables SII, SVII, SXII), bond angles (Tables SIII, SVIII, SXIII), and thermal parameters (Tables SIV, SIX, SXIV) for compounds **3**, **5**, and **6**, respectively (24 pages); listings of observed and calculated structure factors for **3**, **5**, and **6** (32 pages). Ordering information is given on any current masthead page.

---

(20) Cromer, D. T.; Waber, J. T. *International Tables for X-ray Crystallography*; The Kynoch Press: Birmingham, U.K., 1974; Vol. IV.

Reactions of $(OC)_{4,3}Mn^-$ and $(OC)_{3,2}Fe^{\bullet-}$ with Alkenes, Dienes, Acetylene, and Benzene: Ground Electronic States of the Negative Ions

Richard N. McDonald,* Michael T. Jones, and A. Kasem Chowdhury

Department of Chemistry, Kansas State University, Manhattan, Kansas 66506

Received April 25, 1991

$(OC)_4Mn^-$ and $(OC)_3Fe^{\bullet-}$ react with propene, 1,3-butadiene, cyclopentadiene, and benzene exclusively by η^2 addition, while allene and acetylene effect substitution competitive with addition. The high-spin triplet ground electronic state of $(OC)_4Mn^-$ is assigned on the basis of the slow rates for these reactions and its isoelectronic relationship with $Fe(CO)_4$, a triplet ground-state species. The reactions of the doubly unsaturated ions $(OC)_3Mn^-$ and $(OC)_2Fe^{\bullet-}$ ($(OC)_xM^-$) with propene and benzene form saturated adduct product ions assigned as $(OC)_xM(H)(\eta^3\text{-}C_3H_5)^-$ and $(OC)_xM(\eta^4\text{-}C_6H_6)^-$, respectively. The $(OC)_xM^-$ ions react with 1,3-butadiene to give adduct and (adduct – CO) products via excited η^4-diene intermediates. The latter branching fractions depend on the collisional quenching efficiency of the excited intermediates and the unimolecular rate of CO loss. With cyclopentadiene, the $(OC)_xM^-$ ions yield the corresponding (adduct – CO) products characterized as the $(OC)_{x-1}M(H)(\eta^5\text{-c-}C_5H_5)^-$ ions. The reactions of the $(OC)_xM^-$ ions with acetylene occur exclusively by ligand substitution terminating in the formation of the $M(C_2H_2)_x^-$ products, where M = Mn, $x = 3$, and M = Fe, $x = 2$. These product ions and the intermediate $(OC)Mn(C_2H_2)_2^-$ are shown to be the acetylene complexes rather than the corresponding metallacycles.

Inter- and intramolecular C–H bond activation studies continue to be an area of considerable interest in the chemistry of coordinatively and electronically unsaturated organometallic intermediates.[1] In the condensed phase, it has been particularly intriguing that oxidative insertion of various metal centers occurs with cyclopropyl, olefinic, and aromatic C–H bonds that have large dissociation energies.[2,3] In these reactions, the sum of the M–H and M–R bonds formed must exceed the energy of the R–H bond broken and the unfavorable entropy of the insertion process. Considerably stronger M–phenyl vs M–alkyl bonds have been observed in the $Cp^*(Me_3P)M(H)(R)$ complexes where M = Ir[4,5] or Rh[6] and $Cp^* = \eta^5\text{-}C_5Me_5$; in the iridium complex, $D°(Ir–H) = 74.2$ kcal mol^{-1} and $D°$(Ir–phenyl) = 80.6 kcal mol^{-1}.[5]

It has been assumed that the ready oxidative insertion reactions into C–H bonds of alkenes and aromatics occur by prior coordination of the metal center with the π electrons followed by the oxidative insertion step.[1j,o,p,r,6,7]

---

(1) For reviews of this topic, see: (a) Ryabov, A. D. *Chem. Rev.* **1990,** *90,* 403. (b) Halpern, J. *Inorg. Chim. Acta* **1985,** *57,* 1897. (c) Crabtree, R. H. *Chem. Rev.* **1985,** *85,* 245. (d) Green, M. L. H.; O'Hare, D. *Pure Appl. Chem.* **1985,** *57,* 1897. (e) Rothwell, I. P. *Polyhedron* **1985,** *4,* 177. (f) Shilov, A. E. *The Activation of Saturated Hydrocarbons by Transition Metal Complexes*; Reidel: Dordrecht, The Netherlands, 1984. (g) Parshall, G. W. *Chem. Tech.* **1984,** *14,* 628. (h) Muetterties, E. L. *Chem. Soc. Rev.* **1983,** *12,* 283. (i) Brookhart, M.; Green, M. L. H. *J. Organomet. Chem.* **1983,** *250,* 395. (j) Somorjai, G. *Chemistry in Two Dimensions*; Cornell University Press: Ithaca, NY, 1981. (k) Parshall, G. W. *Homogeneous Catalysis*; Wiley: New York, 1980. (l) James, B. R. *Homogeneous Hydrogenation*; Wiley: New York, 1980; Chapter 7. (m) Muetterties, E. L.; Rhodin, T. N.; Band, E.; Brucker, C. F.; Pretzer, W. R. *Chem. Rev.* **1979,** *79,* 91. (n) Webster, D. E. *Adv. Organomet. Chem.* **1977,** *15,* 147. (o) Parshall, G. W. In *Catalysis; Specialist Periodical Report*; The Chemical Society: London, 1977; Vol. 1, 335. (p) Parshall, G. W. *Acc. Chem. Res.* **1975,** *8,* 113. (q) Parshall, G. W. *Homogeneous Hydrogenation*; Wiley: New York, 1973. (r) Parshall, G. W. *Catalysis* **1972,** *1,* 335. (s) Parshall, G. W. *Acc. Chem. Res.* **1970,** *3,* 139. (t) Halpern, J. *Acc. Chem. Res.* **1970,** *3,* 386. (u) Collman, J. P. *Acc. Chem. Res.* **1968,** *1,* 136.

(2) Baghal-Vayjooee, M. H.; Benson, S. W. *J. Am. Chem. Soc.* **1979,** *101,* 2838. $D°(c\text{-}C_3H_5–H) = 106.3 \pm 0.25$ kcal mol^{-1}.

(3) Benson, S. W. *Thermochemical Kinetics*, 2nd ed.; Wiley: New York, 1976; p 309. $D°(H_2C{=}CH–H) = 108$ kcal mol^{-1}, $D°(C_6H_5–H) = 110.5$ kcal mol^{-1}, and $D°(H_2C{=}CHCH_2–H) = 87$ kcal mol^{-1}.

(4) Buchanan, J. M.; Stryker, J. M.; Bergman, R. G. *J. Am. Chem. Soc.* **1986,** *108,* 1537.

(5) Nolan, S. P.; Hoff, C. D.; Stoutland, P. O.; Newman, L. J.; Buchanan, J. M.; Bergman, R. G.; Yang, G. K.; Peters, K. S. *J. Am. Chem. Soc.* **1987,** *109,* 3143.

(6) Jones, W. D.; Feher, F. J. *J. Am. Chem. Soc.* **1984,** *106,* 1650.

0276-7333/92/2311-0392$03.00/0

However, Stoutland and Bergman[8] demonstrated that the hydrido–vinyl complex $(\eta^5\text{-}C_5Me_5)(Me_3P)Ir(H)(CH{=}CH_2)$ formed in the reaction of $(\eta^5\text{-}C_5Me_5)Ir(PMe_3)$ with ethylene is not produced via the π complex. Jones and Feher[6] have shown that η^2-arene complexes are implicated as intermediates in the oxidative insertion reactions of $(\eta^5\text{-}C_5Me_5)Rh(PMe_3)$ into arene C–H bonds using kinetic and comparative inter- and intramolecular isotope effect studies.

Our recent reports of adduct formation in the gas-phase C–H bond oxidative insertion reactions of $(OC)_2Fe^{\bullet-}$ with methane and 2,2-dimethylpropane[9] and of $(OC)_2Fe^{\bullet-}$ and $(OC)_3Mn^-$ with cyclopropane[10] requires that the sum of the new bonding in the $(OC)_2Fe(H)(R)^{\bullet-}$ anionic products is greater than $D°(R\text{–}H)$ for these hydrocarbons. This conclusion also extends to the dehydrogenation reactions by $(OC)_2Fe^{\bullet-}$ and $(OC)_3Mn^-$ with a series of *n*-alkanes, cyclopentane, and cyclohexane.[9] Thus, the M–H and M–R dissociation energies in the unsaturated anionic metal complexes may be greater than those in the saturated first-row neutral complexes. Dissociation energies for some neutral coordinatively saturated first-row M–alkyl ($\approx$30 kcal mol^{-1}) and M–hydride ($\approx$60 kcal mol^{-1}) bonds are becoming available.[11]

The purpose of the present study was to determine if C–H bond activation would compete with or sequentially follow π coordination of various unsaturated organic molecules, i.e. olefins, dienes, acetylene, and benzene, to $(OC)_3Mn^-$ and $(OC)_2Fe^{\bullet-}$. Although alkene and arene C_{sp^2}–H bond activation is not observed, intramolecular $C_{allylic}$–H bond insertion dominates the reactions with propene and cyclopentadiene. A second feature of the work results from a comparison of the magnitudes of the rate constants for the addition reactions of these organic ligands to $(OC)_4Mn^-$, $(OC)_3Mn^-$, and $(OC)_3Fe^{\bullet-}$. The small rate constants for the $(OC)_4Mn^-$ reactions support the suggested spin multiplicity change[12] in forming these adduct products. The results demonstrate significant differences in the ratios of the reaction efficiencies. These differences may reflect the curve crossing efficiencies of the triplet–singlet potential energy curves for the forbidden $(OC)_4Mn^-$ addition reactions that depend on the structure of the neutral reactant.

Experimental Section

The gas-phase studies are carried out in a previously described flowing afterglow (FA) apparatus at 298 K.[13] The conditions have been described to separately generate $(OC)_4Fe^{\bullet-}$ and $(OC)_5Mn^-$ and mixtures of $(OC)_{4,3}Fe^{\bullet-}$ or $(OC)_{4,3,2}Fe^{\bullet-}$ and $(OC)_{5,4}Mn^-$ or $(OC)_{5,4,3}Mn^-$ by dissociative attachment of electrons of different energies with $Fe(CO)_5$ and $Mn_2(CO)_{10}$, respectively, in a fast flow of helium buffer gas ($P_{He} \approx 0.9$ Torr, $\bar{v} \approx 57$ m s^{-1}).[9] With these three sets of conditions, the separate chemistry of each ion in the groups can be determined. Variations in P_{He} in these experiments are very limited in order to maintain the ion signals of the mixtures of $(OC)_{4,3,2}Fe^{\bullet-}$ and $(OC)_{5,4,3}Mn^-$ formed using the most energetic ion/electron plasma conditions. It is fortunate that the relatively high P_{He}, which is necessary to afford the signals of these two ion mixtures, facilitates observation of adduct products formed in several of their reactions.

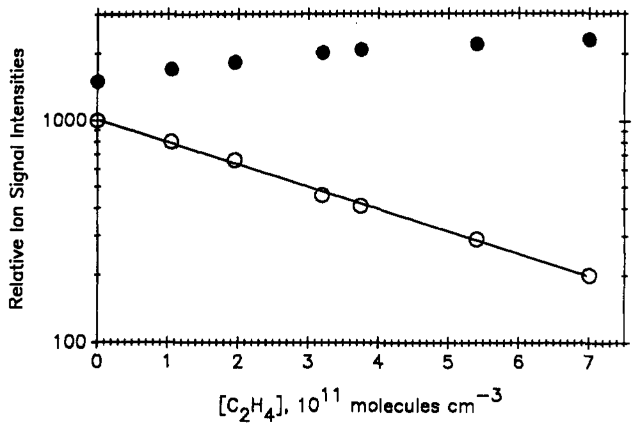

Figure 1. Plot of log [ion signals] vs [N] for the reaction of $(OC)_3Mn^-$ (○) with ethylene forming the adduct $(OC)_4Mn(\pi\text{-}C_2H_4)^-$ (●) at *m/z* 167. $(OC)_4Mn^-$ (●) also at *m/z* 176 does not react with ethylene under these conditions.

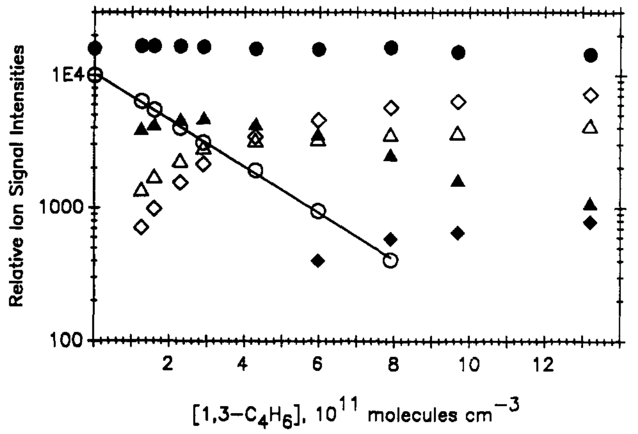

Figure 2. Plot of log [ion signals] vs [N] for the reaction of $(OC)_3Mn^-$ (○) with 1,3-butadiene forming the ion products at *m/z* 193 (△), 165 (▲), 219 (◇), and 191 (◆) ($(OC)_4Mn^-$ (●)).

The initially formed excited fragment metal carbonyl ions are collisionally quenched to give the ions in their electronic and vibrational ground states by multiple collisions with the helium buffer gas in their flight down the first 75 cm of the flow tube. The gaseous neutrals are added via a radial inlet, and the ion/molecule reactions occur in the final 65 cm of the flow tube. The constant flow is maintained by a large, fast-pumping system. The flow is sampled via 1-mm orifices in two nose cones into a differentially pumped chamber ($P \approx 10^{-7}$ Torr) containing a quadrupole mass filter and electron multiplier that continuously monitor the ion composition of the flow. The neutral products of these reactions are not directly observed but are assumed on the basis of thermochemistry and mass balance. Endothermic reactions are not observed in these gas-phase reactions.

The kinetics of these bimolecular reactions are determined under pseudo-first-order conditions where the concentration of the neutral reactant, [N], is always in large excess compared to the ion concentration. In our experiments, the reaction distance, which is directly related to reaction time, is held as a constant while [N] is varied. The slopes, d(log $[Ion^-]$)/d[N], of the plots of log [starting ion signal] vs increasing [N] added to the flow yield the bimolecular rate constants by equations already given.[13b] The FA allows the determination of rate constants for reactions that occur on every collision ($k \approx 10^{-9}$ cm^3 molecule^{-1} s^{-1}) to those that occur in one out of every 10 000 collisions ($k = 10^{-13}$ cm^3 molecule^{-1} s^{-1}).

---

(7) (a) Fryzuk, M. D.; Jones, T.; Einstein, F. W. D. *Organometallics* **1984**, *3*, 185. (b) Nubel, P. O.; Brown, T. L. *J. Am. Chem. Soc.* **1984**, *106*, 644. (c) Jones, W. D.; Feher, F. J. *J. Am. Chem. Soc.* **1982**, *104*, 4240. (d) Muetterties, E. L.; Bleeke, J. R. *Acc. Chem. Res.* **1979**, *12*, 324. (e) Keister, J. B.; Shapley, J. R. *J. Organomet. Chem.* **1975**, *85*, C29. (f) Chatt, J.; Davidson, J. M. *J. Chem. Soc.* **1965**, 843.

(8) (a) Stoutland, P. O.; Bergman, R. G. *J. Am. Chem. Soc.* **1985**, *107*, 4581. (b) Stoutland, P. O.; Bergman, R. G. *J. Am. Chem. Soc.* **1988**, *110*, 5732.

(9) McDonald, R. N.; Jones, M. T.; Chowdhury, A. K. *J. Am. Chem. Soc.* **1991**, *113*, 476.

(10) McDonald, R. N.; Jones, M. T.; Chowdhury, A. K. *J. Am. Chem. Soc.*, in press.

(11) Halpern, J. *Acc. Chem. Res.* **1982**, *15*, 238.

(12) McDonald, R. N.; Jones, M. T.; Chowdhury, A. K. *Organometallics*, in press.

(13) (a) McDonald, R. N.; Chowdhury, A. K. *J. Am. Chem. Soc.* **1985**, *107*, 4123. (b) McDonald, R. N.; Chowdhury, A. K.; Setser, D. W. *Ibid.* **1980**, *102*, 6491.

Table I. Summary of Kinetic and Primary Product Data for the Reactions of $(OC)_4Mn^-$ with Unsaturated Hydrocarbons

reacn no.	neutral reactant	product ion [+ assumed neutral(s)]	branching fraction	$k_{tot.}$,[a] cm^3 molecule^{-1} s^{-1}	k_{LAN},[b] cm^3 molecule^{-1} s^{-1}	reacn efficiency[c]
1	$H_2C{=}CH_2$	$(OC)_4Mn(\eta^2\text{-}C_2H_4)^-$	1.00	$(1.8 \pm 0.1) \times 10^{-12}$[d]	9.8×10^{-10}	0.0018
2	$CH_3CH{=}CH_2$	$(OC)_4Mn(\eta^2\text{-}C_3H_6)^-$	1.00	$(4.0 \pm 0.3) \times 10^{-12}$[d]	1.0×10^{-9}	0.0040
3a	$H_2C{=}C{=}CH_2$	$(OC)_4Mn(C_3H_4)^-$	0.89	$(8.6 \pm 0.9) \times 10^{-12}$	1.0×10^{-9}	0.0086
3b		$(OC)_3Mn(C_3H_4)^-$ [+CO]	0.11			
4	$H_2C{=}CHCH{=}CH_2$	$(OC)_4Mn(\eta^2\text{-}C_4H_6)^-$	1.00	$(1.6 \pm 0.2) \times 10^{-11}$[d]	1.0×10^{-9}	0.016
5	$c\text{-}C_5H_6$	$(OC)_4Mn(\eta^2\text{-}c\text{-}C_5H_6)^-$	1.00	$(9.5 \pm 0.7) \times 10^{-12}$[d]	1.0×10^{-9}	0.0095
6a	$HC{\equiv}CH$	$(OC)_4Mn(C_2H_2)^-$	0.76	$(6.4 \pm 0.8) \times 10^{-12}$	9.0×10^{-10}	0.0071
6b		$(OC)_3Mn(C_2H_2)^-$ [+CO]	0.24			
7	C_6H_6	$(OC)_4Mn(\eta^2\text{-}C_6H_6)^-$	1.00	$(6.4 \pm 0.2) \times 10^{-12}$[d]	1.0×10^{-9}	0.0064

[a] These values are averages of at least two separate measurements. The listed errors are the maximum deviations in the measured rate constants from this average value, which is generally <±10%. The errors due to systematic uncertainties in calibrations suggest that their accuracy is ±20% for external comparisons. [b] Langevin collision limited rate constants; see ref 14. [c] Defined as $k_{tot.}/k_{LAN}$. [d] k_{app} for the formally termolecular adduct-forming reaction.

Table II. Summary of Kinetic and Primary Product Data for the Reactions of $(OC)_3Mn^-$ with Unsaturated Hydrocarbons

reacn no.	neutral reactant	product ion [+ assumed neutral(s)]	branching fraction	$10^{10}k_{tot.}$,[a] cm^3 molecule^{-1} s^{-1}	k_{LAN},[b] cm^3 molecule^{-1} s^{-1}	reacn efficiency[c]
1	$H_2C{=}CH_2$	$(OC)_3Mn(C_2H_4)^-$	1.00	3.1 ± 0.3[d]	1.0×10^{-9}	0.31
2	$CH_3CH{=}CH_2$	$(OC)_3Mn(H)(\eta^3\text{-}C_3H_5)^-$	1.00	3.8 ± 0.3[d]	1.0×10^{-9}	0.38
3	$CD_3CD{=}CD_2$	$(OC)_3Mn(D)(\eta^3\text{-}C_3D_5)^-$	1.00	3.2 ± 0.3[d]		0.32
4	$CD_3CH{=}CH_2$	$(OC)_3Mn(D)(\eta^3\text{-}C_3H_3D_2)^-$	1.00	3.3 ± 0.3[d]		0.33
5a	$H_2C{=}CHCH{=}CH_2$	$(OC)_3Mn(\eta^4\text{-}C_4H_6)^-$	0.28	6.8 ± 0.1	1.1×10^{-9}	0.62
5b		$(OC)_2Mn(\eta^4\text{-}C_4H_6)^-$ [+CO]	0.72			
6	$c\text{-}C_5H_6$	$(OC)_2Mn(H)(\eta^5\text{-}C_5H_5)^-$ [+CO]	1.00	6.7 ± 0.3	1.1×10^{-9}	0.61
7	$HC{\equiv}CH$	$(OC)_2Mn(C_2H_2)^-$ [+CO]	1.00	4.6 ± 0.2	9.1×10^{-10}	0.51
8	C_6H_6	$(OC)_3Mn(\eta^4\text{-}C_6H_6)$	1.00	6.2 ± 0.2[d]	1.1×10^{-9}	0.56

[a–d] See Table I.

Table III. Summary of Kinetic and Primary Product Data for the Reactions of $(OC)_3Fe^{\bullet-}$ with Unsaturated Hydrocarbons

reacn no.	neutral reactant	product ion [+ assumed neutral(s)]	branching fraction	$10^{10}k_{tot.}$,[a] cm^3 molecule^{-1} s^{-1}	k_{LAN},[b] cm^3 molecule^{-1} s^{-1}	reacn efficiency[c]
1	$CH_3CH{=}CH_2$	$(OC)_3Fe(\eta^2\text{-}C_3H_6)^{\bullet-}$	1.00	3.7 ± 0.3[d]	1.0×10^{-9}	0.37
2a	$H_2C{=}C{=}CH_2$	$(OC)_3Fe(C_3H_4)^{\bullet-}$	0.48	4.8 ± 0.4	1.0×10^{-9}	0.48
2b		$(OC)_2Fe(C_3H_4)^{\bullet-}$ [+CO]	0.52			
3a	$H_2C{=}CHCH{=}CH_2$	$(OC)_3Fe(\eta^2\text{-}C_4H_6)^{\bullet-}$	0.98	4.6 ± 0.5[d]	1.1×10^{-9}	0.42
3b		$(OC)_2Fe(\eta^4\text{-}C_4H_6)^{\bullet-}$ [+CO]	0.02			
4	$c\text{-}C_5H_6$	$(OC)_3Fe(\eta^2\text{-}c\text{-}C_5H_6)^{\bullet-}$	1.00	4.8 ± 0.3[d]	1.1×10^{-9}	0.44
5	$HC{\equiv}CH$	$(OC)_2Fe(C_2H_2)^{\bullet-}$ [+CO]	1.00	2.3 ± 0.3	9.1×10^{-10}	0.25
6	C_6H_6	$(OC)_3Fe(\eta^2\text{-}C_6H_6)^{\bullet-}$	1.00	5.2 ± 0.4[d]	1.1×10^{-9}	0.47

[a–d] See Table I.

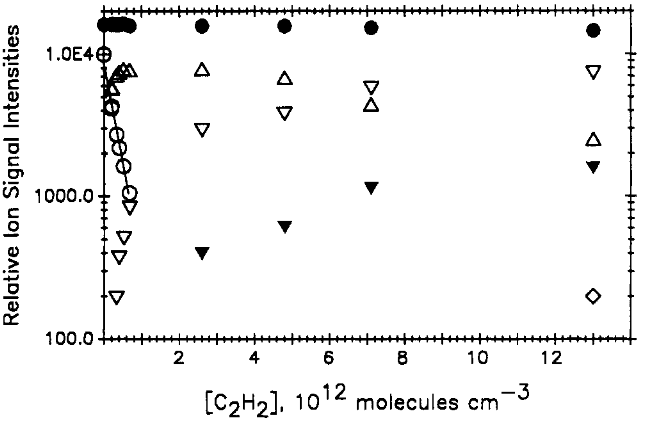

Figure 3. Plot of log [ion signals] vs [N] for the reaction of $(OC)_3Mn^-$ (●) with acetylene forming the ligand substitution products $(OC)_2Mn(C_2H_2)^-$ (△), $(OC)Mn(C_2H_2)_2^-$ (▽), and $Mn(C_2H_2)_3^-$ (▼). Only with the largest concentration of acetylene added is a decrease in the ion signal of $(OC)_4Mn^-$ (●) observed concomitant with formation of the adduct $(OC)_4Mn(\pi\text{-}C_2H_2)^-$ (◇).

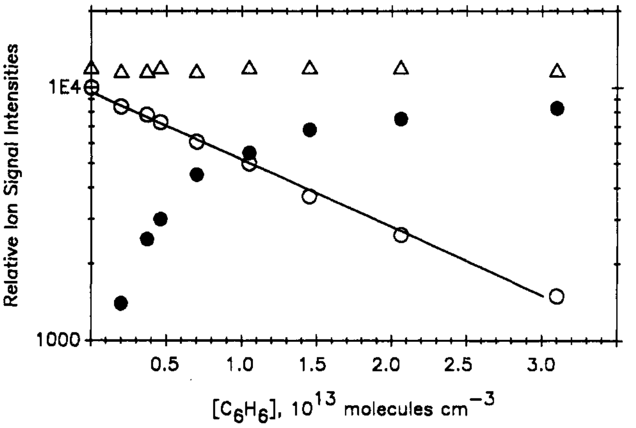

Figure 4. Plot of log [ion signals] vs [N] for the reaction of $(OC)_4Mn^-$ (●) with benzene yielding the adduct ions $(OC)_4Mn(\eta^2\text{-}C_6H_6)^-$ (●) ($(OC)_5Mn^-$ (△)).

Results

The 18-electron $(OC)_5Mn^-$ and 17-electron $(OC)_4Fe^{\bullet-}$ complex ions did not react with any of the neutral reactants used in this study. The kinetic and primary product data for the reactions of $(OC)_{4,3}Mn^-$ and of $(OC)_{3,2}Fe^{\bullet-}$ with the neutrals are given in Tables I–IV. In all of the experiments, linear pseudo-first-order decay plots of the starting ions were observed in the log [ion signal intensities] vs concentrations of the added neutral substrate. Examples of these data plots are shown in Figures 1–4. The product ion signal intensities accounted for >90% of

Table IV. Summary of Kinetic and Primary Product Data for the Reactions of $(OC)_2Fe^{\bullet -}$ with Unsaturated Hydrocarbons

reacn no.	neutral reactant	product ion [+ assumed neutral(s)]	branching fraction	$10^{10}k_{tot.}$,[a] cm^3 molecule^{-1} s^{-1}	k_{LAN},[b] cm^3 molecule^{-1} s^{-1}	reacn efficiency[c]
1	$CH_3CH{=}CH_2$	$(OC)_2Fe(H)(\eta^3\text{-}C_3H_5)^{\bullet -}$	1.00	3.3 ± 0.2[d]	1.0×10^{-9}	0.33
2a	$H_2C{=}CHCH{=}CH_2$	$(OC)_2Fe(\eta^4\text{-}C_4H_6)^{\bullet -}$	0.71	6.2 ± 0.4	1.1×10^{-9}	0.56
2b		$(OC)Fe(\eta^4\text{-}C_4H_6)^{\bullet -}$ [+CO]	0.29			
3	c-C_5H_6	$(OC)Fe(H)(\eta^5\text{-c-}C_5H_5)^{\bullet -}$ [+CO]	1.00	5.4 ± 0.1	1.1×10^{-9}	0.49
4	$HC{\equiv}CH$	$(OC)Fe(C_2H_2)^{\bullet -}$ [+CO]	1.00	4.6 ± 0.1	9.3×10^{-10}	0.49
5	C_6H_6	$(OC)_2Fe(\eta^4\text{-}C_6H_6)^{\bullet -}$	1.00	6.4 ± 0.4[d]	1.1×10^{-9}	0.58

[a–d] See Table I.

the loss of the starting ion signal. The branching fractions given in Tables I–IV and in equations in the Discussion are the relative product ion signal intensities obtained by integration of the negative ion spectra (averages of 10–15 spectra to increase signal-to-noise ratios) taken for 6–10 different concentrations of the added neutral reactant. The error in these branching fractions is ±3% absolute within the number of kinetic runs used to determine the average rate constant.

Several of these reactions yield adduct product ions. In these reactions, removal of the excess energy in forming the adduct structure is required by collisions with the helium buffer gas or the adduct will dissociate. The apparent bimolecular rate constants, k_{app}, are reported herein for these formally termolecular reactions due to our inability to significantly vary P_{He}. However, the rate constants listed in Tables II–IV exceed 30% of the Langevin collision-limited rate constant, k_{LAN},[14] for the present adduct and/or substitution product forming reactions. This illustrates that the present conditions are either at or very close to the high-pressure limit for these processes. Thus, the reactivity comparisons of different metal carbonyl negative ions with the same neutral substrate using the measured k_{app} will show no to little change with increasing P_{He}.

In the comparisons of the reactivities of the four fragment metal carbonyl negative ions with the neutrals, the reaction efficiencies (RE) will be used. The RE values are defined as $k_{tot.}$ or k_{app} divided by k_{LAN}[14] that correct the measured rate constants for the different polarizabilities of the neutrals and the masses of the neutrals and the ions.

Discussion

Reactions with Alkenes. The stable ethylene complex $(OC)_3Mn(\pi\text{-}C_2H_4)^-$ was observed as the exclusive product in the dehydrogenation of ethane with $(OC)_3Mn^-$.[9] It was possible that the H_2 ejected from the proposed excited intermediate $[(OC)_3Mn(H)_2(\pi\text{-}C_2H_4)^-]^*$ could carry off sufficient excess energy to stabilize the product. Thus, it was of interest for comparing bond strengths in these negative ion complexes to see if the coordination of the alkene would produce the adduct or the product of CO substitution.

The addition of ethylene to $(OC)_4Mn^-$ occurred slowly to produce the corresponding adduct at m/z 195 (eq 1); the $(OC)_{5,4}Mn^-$ ion mixture used contained >2% $(OC)_3Mn^-$.

$$\underset{m/z\ 167}{(OC)_4Mn^-} + H_2C{=}CH_2 \xrightarrow{He} \underset{m/z\ 195}{(OC)_4Mn(\pi\text{-}C_2H_4)^-} \quad (1)$$

Since ethylene has a molecular weight of 28, the same as CO at unit mass resolution of the quadrupole mass filter, this is the same mass as the $(OC)_5Mn^-$ ions that are also present in the flow. The increase in the integrated signal intensity at m/z 195 was equal to the attenuation of the intensity of the ion signal at m/z 167. Using ethylene-d_4 clearly showed the generation of the product ions at m/z 199. We assume that the ethylene π complexes are formed.

The reaction of $(OC)_3Mn^-$ with ethylene was 172 times faster than reaction 1 and produced the corresponding adduct (eq 2). This was accompanied by the concomitant

$$\underset{m/z\ 139}{(OC)_3Mn^-} + H_2C{=}CH_2 \xrightarrow{He} \underset{m/z\ 167}{(OC)_3Mn(\pi\text{-}C_2H_4)^-} \quad (2)$$

increase in the ion signal at m/z 167 initially due to the $(OC)_4Mn^-$ ions in the flow mixture and accounted for >95% of the product ions from reaction 2. The data for reaction 2 are plotted in Figure 1. The ion/molecule chemistry of these ethylene-adduct product ions is identical to that for these same ions obtained as the dehydrogenation products from the reaction of $(OC)_3Mn^-$ with ethane.[9] They underwent at least three H/D exchanges with D_2 ($k_{tot.} = (1.6 \pm 0.2) \times 10^{-11}$ cm^3 molecule^{-1} s^{-1})[15] and formed adducts with Me_3SiH and SiH_4,[12] and SO_2 effected ligand substitution with formation of $(OC)_3Mn(SO_2)^-$ ($k_{tot.} = (9.6 \pm 0.9) \times 10^{-10}$ cm^3 molecule^{-1} s^{-1}; RE[16] = 0.87). These results characterized these ions as the 16-electron π-ethylene complexes. The failure of these complexes to add a second ethylene ligand is probably the result of a spin multiplicity change in $(OC)_3Mn(\pi\text{-}C_2H_4)^-$ going to $(OC)_3Mn(\pi\text{-}C_2H_4)_2^-$ (to be discussed later) and possibly steric crowing.

The reactions of $(OC)_{3,2}Fe^{\bullet -}$ with ethylene were not examined.

Both $(OC)_4Mn^-$ and $(OC)_3Fe^{\bullet -}$ reacted with propene to form the adducts which are assumed to be the corresponding π complexes (eq 3). As in the above reactions

$$(OC)_xM^- + CH_3CH{=}CH_2 \xrightarrow{He} (OC)_xM(\pi\text{-}C_3H_6)^- \quad (3)$$
$$M = Mn,\ x = 4;\ M = Fe,\ x = 3$$

of $(OC)_{4,3}Mn^-$ with ethylene, the binding energy of the alkenes to the fragment metal carbonyl negative ions is not large enough to effect release of a CO ligand from the adduct product relative to collisional quenching. It is interesting that the rate constant for reaction 3 between $(OC)_3Fe^{\bullet -}$ and propene is 93 times larger than that for the analogous reaction with $(OC)_4Mn^-$.

The fast reactions of the doubly unsaturated anions $(OC)_3Mn^-$ and $(OC)_2Fe^{\bullet -}$ with propene also formed the adducts according to eq 4. These are the same product

$$(OC)_xM^- + CH_3CH{=}CH_2 \xrightarrow{He} (OC)_xM(H)(\eta^3\text{-}C_3H_5)^- \quad (4)$$
$$M = Mn,\ x = 3;\ M = Fe,\ x = 2$$

---

(14) Su, T.; Bowers, M. T. In *Gas Phase Ion Chemistry*; Bowers, M. T., Ed.; Academic Press: New York, 1979; Vol. 1, Chapter 3.

(15) The slow ($k_{app} = (8.6 \pm 1.4) \times 10^{-13}$ cm^3 molecule^{-1} s^{-1}) addition of D_2 to the $(OC)_4Mn^-$ ions present in the flow forms the adduct ions at m/z 171. This is the same mass as the π-ethylene adduct ions at m/z 167 that undergo four H/D exchanges.

(16) RE calculated using average dipole orientation theory[14] to calculate the collision limited rate constant, k_{ADO}, due to the dipole moment of SO_2 (1.63 D).

ions observed in the dehydrogenation reactions of these metal carbonyl negative ions with propene.[9] That these ion products are not simple π-alkene complexes is shown in the results of the further ion/molecule reactions of the adduct product ions at m/z 181 from reaction 4 with $(OC)_3Mn^-$. No reaction of the adduct ions was observed with D_2, H_2S,[9] SiH_4, or Me_3SiH,[12] suggesting that the m/z 181 ions are 18-electron species. A relatively slow ligand substitution was observed with SO_2 forming $(OC)_3Mn(SO_2)^-$ (m/z 203) with a rate constant $k_{tot.} = (1.5 \pm 0.2) \times 10^{-11}$ cm^3 molecule^{-1} s^{-1} (RE[16] = 0.014). The RE is 62 times smaller than the RE for the similar substitution of SO_2 with the 16-electron $(OC)_3Mn(\pi\text{-}C_2H_4)^-$ complex formed in reaction 2. The relative inefficiency of the present substitution reaction with SO_2 may be the result of the unfavorable $\Delta G°$ for the rearrangement of $(OC)_3Mn(H)(\eta^3\text{-}C_3H_5)^-$ to $(OC)_3Mn(\pi\text{-}C_3H_6)^-$ in the collision complex with SO_2;[9,17] no reaction was observed between $(OC)_5Mn^-$ and SO_2. These data strongly suggest that the metal center inserts into an allylic C–H bond in the intermediate π-propene complexes forming the hydrido–(η^3-allyl) product ions.[9]

In an effort to examine the H/D scrambling that would have been observed in a collision between the proposed π-propene intermediate and a single D_2 molecule, we have entered the manifold of such a bound complex from a different direction. This is seen in the reaction of $(OC)_3Mn(D)_2^-$ with propene given in eq 5. The $(OC)_3Mn(D)_2^-$ ions are generated in the reaction of the ion mixture $(OC)_{5,4,3}Mn^-$ with D_2, along with the 18-electron ions $(OC)_3Mn(D)_4^-$ and $(OC)_4Mn(D)_2^-$ that do not react with propene.

$$\underset{m/z\ 143}{(OC)_3Mn(D)_2^-} + CH_3CH{=}CH_2 \xrightarrow{0.40} \underset{m/z\ 181}{(OC)_3Mn(H)(\eta^3\text{-}C_3H_5)^-} + D_2 \qquad (5a)$$

$$\xrightarrow{0.39} \underset{m/z\ 182}{(OC)_3Mn(C_3H_5D)^-} + HD \qquad (5b)$$

$$\xrightarrow{0.21} \underset{m/z\ 183}{(OC)_3Mn(C_3H_4D_2)^-} + H_2 \qquad (5c)$$

Considerable H/D scrambling is obvious in the results of reaction 5. A single branch of the suggested mechanism for reaction 5 is shown in Scheme I following initial π coordination of propene forming **1**. The elimination of D_2 from **1** must be competitive with retro-β-deuterium shifts that favor formation of **2** generating the primary C–D bond. A β-hydrogen shift from the methyl group in **2** yields **3**, which can competitively expel HD or rearrange to **4** where loss of H_2 can occur. The rearrangements of **1** to **3** and of **3** to **4** are energetically favored by the difference in zero-point energy (ΔZPE) in converting Mn–D and C–H bonds in **1** and **3** into Mn–H and C–D bonds in **3** and **4**, respectively.[18] These structures and reversible steps are analogous to those described for the reaction of $(OC)_3Mn(\pi\text{-}C_2H_4)^-$ with D_2 where up to three H/D exchanges in the ethylene ligand were observed.[9]

Simplifying this mechanism to involve only the excited intermediates **1**, **3**, and **4**, we note that the observed ratio of 40:39:21 for the branching fractions of channels 5a:5b:5c involves the partitioning of intermediates **1** and **3** between unimolecular elimination and rearrangement. The equilibrium constants for the rearrangements will be the same (>1), since the same ΔZPE is involved. Since the reaction is predominately in the forward direction, i.e. **1** → **3** → **4**, **1** is partitioned by 0.4 elimination of D_2 and 0.6 rearrangement to **3**. The partitioning of **3** is 0.4 elimination of HD and 0.2 rearrangement to **4** that ejects H_2. This analysis suggests that the ratio of the rate constants for the elimination steps, k_{-D_2}:k_{-HD}:k_{-H_2}, would be approximately 1:2:4.

Scheme I[a]

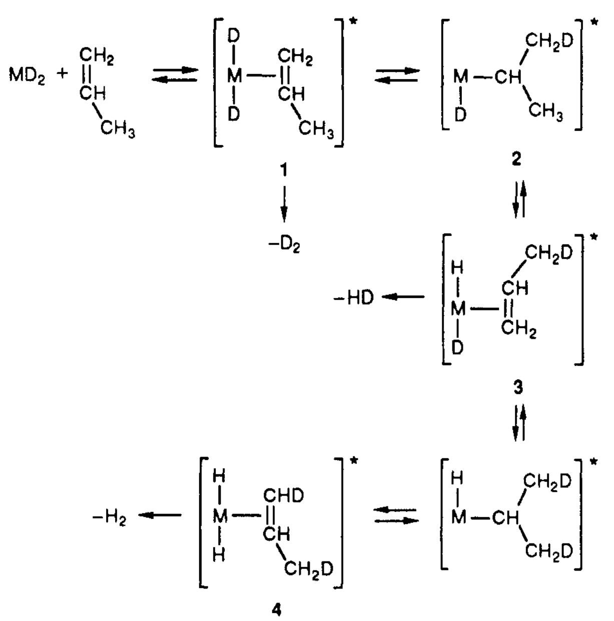

[a] M = $(OC)_3Mn^-$.

It appears that the binding energy of propene in complex **1** is only slightly greater than the binding energy of D_2 in this complex. If the binding energy of propene in complex **1** were much greater than the binding energy of D_2, a larger branching fraction for channel 5a would have been observed. This is the first evidence that the $(OC)_3MnD_2^-$ complex has the metal–dideuteride structure rather than the weaker binding of molecular deuterium to the metal.[18b]

The reactions of $(OC)_3Mn^-$ with the deuterated propene molecules $CD_3CD{=}CD_2$ and $CD_3CH{=}CH_2$ produced the corresponding adducts assigned from the reaction with propene as the corresponding 18-electron hydrido–(η^3-allyl) complexes with the necessary H/D substitutions. The rate constants for the reactions with propene and the deuterated propenes (Table II) are the same within the error limits. A mechanism involving initial π complexation of propene followed by a fast intramolecular insertion of Mn into a C–H bond of the methyl group of the π-bound propene ligand is consistent with this data.

Reactions with Dienes. In the previous section, the absence of CO substitution by ethylene or propene suggested that the binding energy of these alkenes is less than $D°$(M–CO) in the adduct complexes. The reactions of $(OC)_4Mn^-$ and $(OC)_3Fe^{\bullet -}$ with 1,3-butadiene followed a similar course in that adduct formation was the exclusive or major product channel observed (eqs 6 and 7). The minor difference is the small amount of the substitution channel 7b. No further reaction of the products of channel 7b with 1,3-butadiene was observed, suggesting that the diene in these complexes is an η^4-ligand. With 1,3-butadiene, the ratio $RE_7/RE_6 = 29$.

The reactions of $(OC)_4Mn^-$ and $(OC)_3Fe^{\bullet -}$ with cyclopentadiene proceeded in an analogous manner forming the corresponding adducts (eq 8). The presence of the *cis*-

---

(17) Variable-temperature studies that might check this postulate are not possible with our FA.

(18) For the IR stretching frequencies of metal hydride bonds, (a) ν_{MH} 2200–1600 cm^{-1} (Collman, J. P.; Hegedus, L. S.; Norton, J. R.; Finke, R. G. *Principles and Applications of Organotransition Metal Chemistry*; University Science Books: Mill Valley, CA, 1987; p 83) and (b) ν_{MH} 2300–1700 cm^{-1} (Kubas, G. J. *Acc. Chem. Res.* **1988**, *21*, 120).

$$\underset{\underline{m/z}\ 139}{(OC)_4Mn^-} + CH_2{=}CHCH{=}CH_2 \xrightarrow{He} \underset{\underline{m/z}\ 193}{(OC)_4Mn(\pi\text{-}C_4H_6)^-} \tag{6}$$

$$\underset{\underline{m/z}\ 112}{(OC)_3Fe^{\bullet -}} + CH_2{=}CHCH{=}CH_2 \xrightarrow[0.98]{He} \underset{\underline{m/z}\ 166}{(OC)_3Fe(\pi\text{-}C_4H_6)^{\bullet -}} \tag{7a}$$

$$\xrightarrow[0.02]{} \underset{\underline{m/z}\ 138}{(OC)_2Fe(\eta^4\text{-}C_4H_6)^{\bullet -}} + CO \tag{7b}$$

diene structure in cyclopentadiene has little influence on the rate constants and the product-forming channel.

$$(OC)_xM^- + c\text{-}C_5H_6 \xrightarrow{He} (OC)_xM(\eta^2\text{-}c\text{-}C_5H_6)^- \tag{8}$$

$$M = Mn,\ x = 4;\ M = Fe;\ x = 3$$

In the reactions of the doubly unsaturated $(OC)_3Mn^-$ and $(OC)_2Fe^{\bullet -}$ ions with 1,3-butadiene, the diene can function as a η^4-ligand and substantially increase the exothermicity of the reactions compared to the reactions with alkenes. In a related study, Gravelle and Weitz[19] reported that the fast reaction of 1,3-pentadiene with $Cr(CO)_4$ in 5 to ≈50 Torr of argon buffer gas initially formed the highly excited $[(\eta^4\text{-diene})Cr(CO)_4]^*$ adducts. The excited η^4-diene adducts underwent bond scission producing excited $[(\eta^2\text{-diene})Cr(CO)_4]^*$ adducts or were collisionally quenched at high Ar buffer gas pressure to give $(\eta^4\text{-diene})Cr(CO)_4$. The unsaturated $[\eta^2\text{-diene}]Cr(CO)_4]^*$ complexes then formed $(\eta^4\text{-diene})Cr(CO)_4$ via a longer time scale first-order process.

The results of the reactions of $(OC)_3Mn^-$ and $(OC)_2Fe^{\bullet -}$ with 1,3-butadiene are given in eqs 9 and 10. The data

$$\underset{\underline{m/z}\ 139}{(OC)_3Mn^-} + CH_2{=}CHCH{=}CH_2 \xrightarrow[0.28]{He} \underset{\underline{m/z}\ 193}{(OC)_3Mn(\eta^4\text{-}C_4H_6)^-} \tag{9a}$$

$$\xrightarrow[0.72]{} \underset{\underline{m/z}\ 165}{(OC)_2Mn(\eta^4\text{-}C_4H_6)^-} + CO \tag{9b}$$

$$\underline{m/z}\ 165 + CH_2{=}CHCH{=}CH_2 \xrightarrow[0.9]{He} \underset{\underline{m/z}\ 219}{(OC)_2Mn(\eta^4\text{-}C_4H_6)(\eta^2\text{-}C_4H_6)^-} \tag{9c}$$

$$\xrightarrow[0.1]{} \underset{\underline{m/z}\ 191}{(OC)Mn(\eta^4\text{-}C_4H_6)_2^-} + CO \tag{9d}$$

$$\underset{\underline{m/z}\ 112}{(OC)_2Fe^{\bullet -}} + CH_2{=}CHCH{=}CH_2 \xrightarrow[0.71]{He} \underset{\underline{m/z}\ 166}{(OC)_2Fe(\eta^4\text{-}C_4H_6)^{\bullet -}} \tag{10a}$$

$$\xrightarrow[0.29]{} \underset{\underline{m/z}\ 138}{(OC)Fe(\eta^4\text{-}C_4H_6)^{\bullet -}} + CO \tag{10b}$$

$$\underline{m/z}\ 138 + CH_2{=}CHCH{=}CH_2 \xrightarrow[0.8]{He} \underset{\underline{m/z}\ 192}{(OC)Fe(\eta^4\text{-}C_4H_6)(\eta^2\text{-}C_4H_6)^{\bullet -}} \tag{10c}$$

$$\xrightarrow[0.2]{} \underset{\underline{m/z}\ 164}{Fe(\eta^4\text{-}C_4H_6)_2^{\bullet -}} + CO \tag{10d}$$

for reaction 9 are shown in Figure 2. The reactions involve the primary product-forming channels of adduct and (adduct − CO) ion production with similar rate constants and efficiencies. The coordinatively unsaturated (adduct − CO) primary product ions from eqs 9b and 10b undergo slower secondary reactions with 1,3-butadiene to terminate the addition/substitution processes. The rate constant for the reaction of $(OC)_2Mn(\eta^4\text{-}C_4H_6)^-$ with 1,3-butadiene (1.7×10^{-10} cm^3 molecule^{-1} s^{-1}) is calculated from the slope of the decay for the last six data points in Figure 2 for these ions at m/z 165.

Using the mechanism proposed by Gravelle and Weitz[19] as a starting point, the observation of the substitution channels 9b and 10b requires an additional bond scission step for ejection of a CO ligand from the excited adduct. This additional step may be due to the lower buffer gas pressure and the use of helium instead of argon in the FA experiments; both factors reduce the collisional quenching efficiency. The modified mechanism for the formation of the primary products of reactions 9 and 10 is shown in Scheme II.

Scheme II

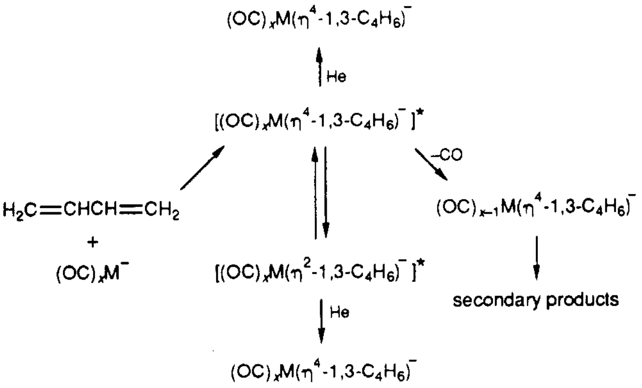

On the basis of this mechanism, the reactions of $(OC)_3Mn^-$ and $(OC)_2Fe^{\bullet -}$ with cyclopentadiene were expected to occur with an increase in the extent of decarbonylation due to the stronger M–(η^4-diene) binding in the cyclopentadiene adducts than in the 1,3-butadiene adducts. The larger electron-donor ability of cyclopentadiene compared to 1,3-butadiene is seen in the lower ionization potential (ΔIP = 12 kcal mol^{-1})[20] and greater proton affinity (ΔPA = 7 kcal mol^{-1})[21] of cyclopentadiene. The raising of the energy of the HOMO in cyclopentadiene reduces the LUMO energy for increased M–diene back-bonding relative to 1,3-butadiene. The sum of these factors leads to an increase in the chemical activation of the $[(OC)_xM(\eta^4\text{-}c\text{-}C_5H_6)^-]^*$ adducts that increases the rate of unimolecular dissociation of a CO ligand and reduces the probability for collisional relaxation of the excited adducts.

Both reactions exclusively formed the corresponding (adduct − CO) ions (eq 11) with the same large rate con-

$$(OC)_xM^- + c\text{-}C_5H_6 \rightarrow (OC)_{x-1}M(H)(\eta^5\text{-}c\text{-}C_5H_5)^- + CO \tag{11}$$

$$M = Mn,\ x = 3;\ M = Fe,\ x = 2$$

stants and efficiencies as those determined for the corresponding reactions with 1,3-butadiene. The (adduct − CO) product ions at m/z 150 (M = Fe, x = 1) and 177 (M = Mn, x = 2) formed in reaction 11 failed to add H_2S[9] or $(CH_3)_3SiH$,[12] insertion reactions that are typically fast with coordinatively unsaturated metal complex negative ions. The (adduct − CO) product ions at m/z 177 (M = Mn, x = 2) *failed to react with* SO_2, an unusual result which previously had only been observed with the 18-electron $(OC)_5Mn^-$ complex.[9] These results demonstrate coordination saturation and the high stability of the metal–organic ligand bonding produced in these reactions. We conclude that the metal centers in the intermediate $[(OC)_{x-1}M(\eta^4\text{-}c\text{-}C_5H_6)^-]^*$ complexes insert into a C–H bond of the methylene group to produce the stable, saturated $(OC)_{x-1}M(H)(\eta^5\text{-}c\text{-}C_5H_5)^-$ complexes. The suggested transformations leading to these product ions are similar in certain respects to those given for the intramolecular

---

[19] Gravelle, S. J.; Weitz, E. *J. Am. Chem. Soc.* **1990**, *112*, 7839.

[20] Rosenstock, H. M.; Draxl, K.; Steiner, B. W.; Herron, J. T. *J. Phys. Chem. Ref. Data, Suppl.* 1977, *6*.

[21] Aue, D. H.; Bowers, M. T. In *Gas Phase Ion Chemistry*; Bowers, M. T., Ed.; Academic Press: New York, 1979; Vol. 2, Chapter 9.

generation of η^5-c-C_5H_5 ligands in condensed phase experiments.[22,23]

The results of the reactions of $(OC)_3Mn^-$ and $(OC)_2Fe^{\bullet-}$ with alkenes and 1,3-butadiene show that $D°(M-CO)$ in the complexes $(OC)_xM(alkene)^-$ ($M = Mn$, $x = 3$; $M = Fe$, $x = 2$) lie between the binding energies of the η^2-alkene and the η^4-1,3-butadiene ligands. It is worthwhile pointing out that the results for the gas-phase reactions of the fragment metal carbonyl species $Cr(CO)_4$, $(OC)_3Mn^-$, and $(OC)_2Fe^{\bullet-}$ with similar acyclic 1,3-dienes can be rationalized by the same mechanism with observed variations attributed to experimental factors.

1,2-Propadiene (allene) with its perpendicular π MOs is an interesting ligand in the present context. The IP of allene is 0.9 eV lower than the IP of ethylene,[20] suggesting that allene will be a better π-donor system. We previously reported the fast exothermic reaction of $(OC)_3Fe^{\bullet-}$ with allene proceeded by competitive addition and substitution (eq 12).[24] Obviously, the exothermicity of binding of the allene to the Fe-metal center exceeds $D°(Fe-CO)$ in the resultant excited adduct. The fragment product ions at m/z 124 added a second allene molecule to form the adduct product at m/z 164.

$$\underset{m/z\ 112}{(OC)_3Fe^{\bullet-}} + CH_2{=}C{=}CH_2 \xrightarrow[0.48]{He} \underset{m/z\ 152}{(OC)_3Fe(\pi\text{-}C_3H_4)^{\bullet-}} \quad (12a)$$

$$\xrightarrow[0.52]{} \underset{m/z\ 124}{(OC)_2Fe(\pi\text{-}C_3H_4)^{\bullet-}} + CO \quad (12b)$$

$$\downarrow CH_2{=}C{=}CH_2$$

$$\underset{m/z\ 164}{(OC)_2Fe(\pi\text{-}C_3H_4)_2^{\bullet-}} \quad (12c)$$

Therefore, it was of interest to examine the analogous reaction with $(OC)_4Mn^-$ to compare branching fractions and rate constants with those of reactions 1, 3, and 12. The results of this reaction are shown in eq 13 and clearly show the increased binding energy of the allene ligand compared to that of an alkene. While similar results were obtained, we note the significant difference in the RE ratio, $RE_{12}/RE_{13} = 54$. The much slower rate of reaction 13 explains why the secondary reaction of the 16-electron fragment ions at m/z 151 with allene was not observed within the time constraints of the FA experiments.

$$\underset{m/z\ 139}{(OC)_4Mn^-} + CH_2{=}C{=}CH_2 \xrightarrow[0.89]{He} \underset{m/z\ 179}{(OC)_4Mn(\pi\text{-}C_3H_4)^-} \quad (13a)$$

$$\xrightarrow[0.11]{} \underset{m/z\ 151}{(OC)_3Mn(\pi\text{-}C_3H_4)^-} + CO \quad (13b)$$

These data likely reduce the magnitude for bracketing $D°(M-CO)$ in these adduct products between the binding energies of ethylene (lower limit) and of allene (upper limit). However, since both binding energies are, as yet, unknown, the need continues for data on bond strengths and other thermodynamic quantities in these transition-metal complex negative ions.

Reactions with Acetylene. Whereas adduct formation was the rule in the reactions of the four unsaturated complex negative ions with propene, the reactions with acetylene all yield the (adduct − CO) product ions. The reaction of $(OC)_4Mn^-$ with acetylene is the only one of the four reactions where both adduct and (adduct − CO) ions are observed as primary products (eq 14). The acetylene ligand in the adduct ions at m/z 165 should be a 2-electron donor to form an 18-electron complex. However, in the (adduct − CO) ions at m/z 137 the acetylene ligand is likely to be a 4-electron donor with the two orthogonal π MOs of the acetylene ligand involved in bonding, since no further reaction of these ions with acetylene was observed. The increased exothermicity of reaction 14 compared to reactions 1 and 3 with the alkenes is established in the expulsion of a CO ligand in eq 14b. However, this greater exothermicity of reaction 14 expresses itself only slightly in a modest increase in RE over the slower, termolecular adduct forming reactions with the two alkenes. Discussion of this and the other slow reactions of $(OC)_4Mn^-$ will be presented in the last part of this section.

$$\underset{m/z\ 139}{(OC)_4Mn^-} + HC{\equiv}CH \xrightarrow[0.76]{He} \underset{m/z\ 165}{(OC)_4Mn(C_2H_2)^-} \quad (14a)$$

$$\xrightarrow[0.24]{} \underset{m/z\ 137}{(OC)_3Mn(C_2H_2)^-} + CO \quad (14b)$$

The results of the fast reaction of the 15-electron complex $(OC)_3Fe^{\bullet-}$ with acetylene are shown in eq 15. If the acetylene ligands in the product ions at m/z 138 were two electron donors, the complexes would be 15-electron species and be expected to add a second acetylene molecule. Since this is not observed, we conclude that the acetylene ligands are 2- or 4-electron donors depending on the electronic demand by the metal center.

$$\underset{m/z\ 112}{(OC)_3Fe^{\bullet-}} + HC{\equiv}CH \rightarrow \underset{m/z\ 138}{(OC)_2Fe(C_2H_2)^{\bullet-}} + CO \quad (15)$$

That π complexation occurs in these reactions rather than C–H bond oxidative insertion is supported by the results observed in the reaction of the 16-electron complex $(OC)_3Mn(D)_2^-$ with acetylene (eq 16). If oxidative insertion into the acetylene C–H bond had occurred, competitive reductive elimination of HD with formation of the product at m/z 166 would have been observed. The idea that the D_2 molecule is completely lost in the ion/neutral collision complex $[((OC)_3Mn(D)_2^-/HC{\equiv}CH) \rightarrow ((OC)_3Mn^-/HC{\equiv}CH) + D_2]^*$ prior to bond-forming steps is incorrect. This conclusion is based on (a) the considerable H/D scrambling observed in the related reaction of this ion with propene (eq 5) illustrating the survival of D_2 in those collision complexes and (b) the expectation of different products from the $[(OC)_3Mn^-/HC{\equiv}CH]$ collision complex (see reaction 17).

$$\underset{m/z\ 143}{(OC)_3Mn(D)_2^-} + HC{\equiv}CH \rightarrow \underset{m/z\ 165}{(OC)_3Mn(C_2H_2)^-} + D_2 \quad (16)$$

The reaction of the 14-electron $(OC)_3Mn^-$ complexes with acetylene is shown in eq 17, and the data are presented in Figure 3. Computer fitting of the data in Figure 3 was carried out to determine the rate constants k_2 and k_3 in reaction 17; $k_1 = k_{tot.}$, the decay constant for $(OC)_3Mn^-$ (Table II).[25] Mass discrimination is not a problem

$$\underset{m/z\ 139}{(OC)_3Mn^-} + HC{\equiv}CH \xrightarrow[k_1]{-CO} \underset{m/z\ 137}{(OC)_2Mn(C_2H_2)^-} \xrightarrow[k_2]{HC\equiv CH} \underset{m/z\ 135}{(OC)Mn(C_2H_2)_2^-} + CO$$

$$k_3 \downarrow HC{\equiv}CH$$

$$\underset{m/z\ 133}{Mn(C_2H_2)_3^-} + CO \quad (17)$$

---

(22) (a) Crabtree, R. H.; Mihelcic, J. M.; Quirk, J. M. *J. Am. Chem. Soc.* **1979**, *101*, 7738. (b) Crabtree, R. H.; Mellea, M. F.; Milhelcic, J. M.; Quirk, J. M. *J. Am. Chem. Soc.* **1982**, *104*, 107.

(23) Crabtree, R. H.; Demou, P. C.; Eden, D.; Milhelcic, J. M.; Parnell, C. P.; Quirk, J. M.; Morris, G. E. *J. Am. Chem. Soc.* **1982**, *104*, 6994.

(24) McDonald, R. N.; Chowdhury, A. K.; Schell, P. L. *J. Am. Chem. Soc.* **1984**, *106*, 6095.

over the seven atomic mass unit range from the starting ions to the final ion product. A good fit of the data in Figure 3 was obtained with $k_2 = 3.5 \times 10^{-11}$ cm^3 molecule^{-1} s^{-1} and $k_3 = 5.0 \times 10^{-12}$ cm^3 molecule^{-1} s^{-1}. Addition of D_2 to the flow containing the mixture of the m/z 137, 135, and 133 ions showed that the m/z 137 ions slowly added D_2 to give an adduct, but no reaction was observed with the ions at m/z 135 and 133.

In reaction 17, the first two ligand substitution reactions probably use the acetylene ligands as 4-electron donors. This would account for the absence of addition of D_2 to the ions at m/z 135. However, the collisions of these m/z 135 ions with an additional strongly binding acetylene molecule must convert one acetylene ligand to a 2-electron donor to accept the third acetylene ligand. The structure of $Mn(C_2H_2)_3^-$ requires one ligand to be a 2-electron donor. The evidence for the above acetylene addition and substitution products is consistent with π-bonding of these ligands rather than oxidative insertion into the C–H bond.

The analogous substitution sequence for the reaction of the 13-electron complex ions $(OC)_2Fe^{\bullet-}$ with acetylene is shown in eq 18 and terminated in the formation of the ion products at m/z 108. As in reaction 17, the rate constant for the secondary reaction of the primary ion product is $\approx 5 \times 10^{-11}$ cm^3 molecule^{-1} s^{-1} determined from the computer fitting of the data.[25] When D_2 was added to the mixture containing the ions m/z 108 and 110, only the ions at m/z 110 reacted to yield its D_2 adduct. This result suggests that the ions at m/z 108 are saturated, 17-electron complexes.

$$\underset{m/z\ 112}{(OC)_2Fe^{\bullet-}} + HC{\equiv}CH \xrightarrow{-CO} \underset{m/z\ 110}{(OC)Fe(C_2H_2)^{\bullet-}} \xrightarrow[-CO]{HC\equiv CH} \underset{m/z\ 108}{Fe(C_2H_2)_2^{\bullet-}} \quad (18)$$

The structures of the product ion complexes in reactions 17 and 18 have the composition of various odd-membered metallacycles or 7-metallanorbonadienes[26] formed in the cyclotrimerization of acetylenes by transition-metal catalysts.[1k,18a] However, the absence of reaction of D_2 with the m/z 133 and 135 products from eq 17 and the m/z 108 products from eq 18 suggest that these ion products are saturated and retain the character of individual acetylene ligands. Thus, the present structures represent certain of the suspected intermediates in the formation of the metallacycles. It appears that additional metal ligation is required to convert the di- or triacetylene complexes into the corresponding metallacycles or 7-metallanorbornadienes,[26] respectively.

Reactions with Benzene. Although benzene usually serves as a 6-electron donor ligand in organometallic complexes in the condensed phase, complexes with benzene as a 2- or 4-electron-donor ligand are known.[18a,26,27] The reactions of $(OC)_4Mn^-$ and $(OC)_3Fe^{\bullet-}$ with benzene produced the corresponding adduct negative ions (eq 19).

$$(OC)_xM^- + C_6H_6 \xrightarrow{He} (OC)_xM(\eta^2\text{-}C_6H_6)^- \quad (19)$$
$$M = Mn,\ x = 4;\ M = Fe,\ x = 3$$

The data for the $(OC)_4Mn^-$ reaction are shown in Figure 4; note the much larger concentrations of neutral required to decay the starting ions compared to those in Figures 1–3. The similarities of the RE for addition of benzene and those of the corresponding reactions with the alkenes, 1,3-butadiene, and cyclopentadiene suggest that π coordination to a "double bond" of the benzene ring occurs.[18a,17] However, the fact that both product ions are saturated 18- and 17-electron complexes, respectively, does not allow for further ion molecule reactions to distinguish between the η^2 structures and the hydrido–phenyl complex.

The corresponding reaction of $(OC)_3MnD_2^-$ with benzene formed the (adduct − D_2), $(OC)_3Mn(\eta^4\text{-}C_6H_6)^-$ at m/z 217, as the exclusive product. This result suggests that the initial step in this reaction is π coordination (η^2) of the metal center to the ring that is sufficiently exothermic to extrude D_2 from the excited 18-electron intermediate adduct. If initial C–H bond insertion had occurred, loss of HD and D_2 would have been expected to be competitive. This result is consistent with the above description given for the reactions shown in eq 19.

Both $(OC)_3Mn^-$ and $(OC)_2Fe^{\bullet-}$ reacted rapidly with benzene to form adduct product ions with similar rate constants and RE values (eq 20). The failure of the product ions of reaction 20 to add Me_3SiH[12] or additional benzene suggests that they have saturated 18- and 17-electron structures, respectively. The product ions from reaction 20, M = Mn, $x = 3$, did react with SO_2 with a modest rate constant ($k_{tot.} = (2.1 \pm 0.4) \times 10^{-11}$ cm^3 molecule^{-1} s^{-1}) to yield the ligand substitution product ions $(OC)_3Mn(SO_2)^-$ by loss of the benzene molecule.

$$(OC)_xM^- + C_6H_6 \xrightarrow{He} (OC)_xM(\eta^4\text{-}C_6H_6)^- \quad (20)$$
$$M = Mn,\ x = 3;\ M = Fe,\ x = 2$$

The absence of (adduct − CO) product forming channels in reactions 20 compared to the abundance of such channels in the diene reactions 10, 11, and 13 is consistent with some of the exothermicity in the η^4-binding of the benzene molecule being offset by the loss of the benzene aromaticity. However, the bond strength $D°((OC)_3Mn^-\text{–}(\eta^4\text{-}C_6H_6))$ must be considerable on the basis of the modest rate constant in the ligand substitution reaction with SO_2.

Comparison of the Reaction Efficiencies for the Reactions of $(OC)_{4,3}Mn^-$ and $(OC)_{3,2}Fe^{\bullet-}$ with Unsaturated Neutrals. The reactions of the 15-electron $(OC)_3Fe^{\bullet-}$ and the 13-electron $(OC)_2Fe^{\bullet-}$ negative ions with the unsaturated neutrals used in this study to yield either adduct or ligand substitution product ions occur with similar large RE values and yield RE ratios close to unity. This is *not* the case for corresponding reactions of the 16-electron $(OC)_4Mn^-$ and 14-electron $(OC)_3Mn^-$ ions where the ratio $RE((OC)_3Mn^-)/RE((OC)_4Mn^-)$ varies from 172 to 39 depending on the ligand (Table V). Similar large values are observed for the $RE((OC)_3Fe^{\bullet-})/RE((OC)_4Mn^-)$ ratios with the same substrate indicating that the degree of coordination unsaturation and changes in the metal center have only minor effects on these rate constants.

The collisional quenching efficiency of the excited adducts $[(OC)_xM(L_u)^-]^*$, where L_u is an unsaturated organic ligand, will be the greatest for M = Mn and $x = 4$ of the four metal carbonyl negative ions used in this study. The larger number of ligands in the excited $[(OC)_4Mn(L_u)^-]^*$

---

[25] Wiberg, K. B. *Physical Organic Chemistry*; Wiley: New York, 1964; pp 321–325 and 570–574. This work describes a program for determining the rate constants for consecutive first-order reactions. The program was extensively modified by Dr. Glenn Lo and uses neutral concentration (for pseudo-first-order reactions) or time as the x-coordinate variable, handles up to 21 consecutive first-order steps, and operates on an IBM-PC computer. The input data are the average ion velocity, the length of the ion/molecule reaction region, $k_1 = k_{tot.}$ and estimates of the other rate constants, the final neutral concentration, and the neutral concentration increments. The values of k_2 and k_3 are adjusted until the calculated and measured plots of relative ion signals vs neutral concentration show good agreement.

[26] Bianchini, C.; Caulton, K. G.; Chardon, C.; Eisenstein, O.; Folting, K.; Johnson, T. J.; Meli, A.; Peruzzini, M.; Rauscher, D. J.; Streib, W. E.; Vizza, F. *J. Am. Chem. Soc.* **1991**, *113*, 5127.

[27] (a) Silverthorn, W. E. *Adv. Organomet. Chem.* **1975**, *13*, 47. (b) Zeiss, H.; Wheatly, P. J.; Winkler, H. J. S. *Benzenoid-Metal Complexes*; Ronald Press: New York, 1966.

Table V. Reaction Efficiency Ratios for the Reactions of $(OC)_4Mn^-$, $(OC)_3Mn^-$, and $(OC)_3Fe^{\bullet-}$ with Neutrals Used in This Study[a]

neutral species	$RE((OC)_3Mn^-)/RE((OC)_4Mn^-)$	$RE((OC)_3Fe^{\bullet-})/RE((OC)_4Mn^-)$
$H_2C{=}CH_2$	172[b]	
$CH_2{=}CHCH_3$	95[b]	93[b]
$H_2C{=}CHCH{=}CH_2$	39[c]	26[b]
c-C_5H_6	64[d]	46[b]
$HC{\equiv}CH$	71[e]	35[f]
C_6H_6	88[b]	73[b]

[a] Data from Tables I–III. [b] Comparing adduct formation with both ions. [c] Comparing adduct + substitution product formation with $(OC)_3Mn^-$ and adduct formation for $(OC)_4Mn^-$. [d] Comparing substitution with $(OC)_3Mn^-$ and adduct formation with $(OC)_4Mn^-$. [e] Comparing substitution with $(OC)_3Mn^-$ and adduct + substitution product formation with $(OC)_4Mn^-$. [f] Comparing substitution with $(OC)_3Fe^{\bullet-}$ and adduct + substitution product formation with $(OC)_4Mn^-$.

adducts increase their density of states and lifetimes[28] that *maximize*, not minimize, the efficiency for collisional relaxation of these adducts. A study of the reaction of $(OC)_3Fe^{\bullet-}$ with ^{13}CO at P_{He} = 1.0 Torr showed the presence of 29% ligand exchange forming $(OC)_2(O^{13}C)Fe^{\bullet-}$ in addition to collisional quenching of the excited intermediate adduct yielding the addition product $(OC)_3(O^{13}C)Fe^{\bullet-}$.[29] The collisional quenching efficiency of the excited adducts $[(OC)_3(O^{13}C)Fe^{\bullet-}]^*$ by helium at 1.0 Torr was 65%. Because of the increased ligation in $[(OC)_4Mn(L_u)^-]^*$, 65% represents a lower limit for the quenching efficiency of these adducts. Thus, the rate constants for the present adduct-forming $(OC)_4Mn^-$ reactions (and those of the other three ions) would only be increased by a small amount if *all* of the excited adducts formed were collisionally quenched.

The above discussion rules out three factors, the degree of coordination unsaturation, Mn vs Fe as the coordinating metal center, and the collisional quenching efficiencies of the ions, as important contributors to the slow rate constants for the $(OC)_4Mn^-$ reactions. We conclude that the poor efficiencies in producing the $(OC)_4Mn(L_u)^-$ adducts are the result of an inherent problem in forming these saturated, 18-electron products. We suggest that *the difference lies in the potential energy surfaces for the ligand addition reactions of $(OC)_4Mn^-$ compared to those of $(OC)_3Mn^-$ and $(OC)_3Fe^{\bullet-}$*. A similar suggestion was made on the basis of the smaller, but significant, RE ratios for the reactions of $(OC)_{4,3}Mn^-$ with trimethylsilane, silane, and germane.[12]

Weitz et al.[30] observed that $Fe(CO)_4$, a high-spin triplet electronic ground-state species with C_{2v} symmetry,[31] only slowly added CO to produce $Fe(CO)_5$, a D_{3h} singlet electronic ground-state complex, in the high-pressure regime of 5 Torr of argon bath gas. The rate constant was about 4 orders of magnitude smaller than the gas kinetic limit. The related reactions of $Fe(CO)_3 + CO \rightarrow Fe(CO)_4$ and of $Fe(CO)_2 + CO \rightarrow Fe(CO)_3$ were fast with rate constants approximately 1 order of magnitude smaller than the gas kinetic limit. Assuming ground-state-to-ground-state processes for these ligand addition reactions, the slow rate for the $Fe(CO)_4 + CO \rightarrow Fe(CO)_5$ reaction was rationalized in terms of the difference in the spin states of the reactants and the products. The fast addition reactions of $Fe(CO)_{3,2}$ with CO appear to proceed on potential energy surfaces of the same spin multiplicity. The results suggest that the three fragment complexes $Fe(CO)_{4,3,2}$ have high-spin triplet electronic ground states.

Since $(OC)_{4,3}Mn^-$ are isoelectronic with the high-spin triplet neutral fragments $Fe(CO)_{4,3}$, it appears reasonable that the two Mn complex negative ions are also high-spin triplet ground-state species. We suggest that the reason for the slow rates of ligand addition reactions with $(OC)_4Mn^-$ is an inefficient crossing from the inlet channel of the triplet ground electronic state for the ion plus the singlet neutral to the exit channel of the singlet ground state of the 18-electron adduct product ions. The fast addition reactions of $(OC)_3Mn^-$ with neutral unsaturated ligands occur on surfaces of the same spin multiplicity.

The negative ions $(OC)_{4,3,2}Fe^{\bullet-}$ are isoelectronic with the $Co(CO)_{4,3,2}$ fragments, and the latter neutrals are known to be low-spin doublet ground-state species.[32,33] This relationship suggests that the three iron carbonyl anion radicals also have low-spin doublet electronic ground states. This accounts for the similar fast ligand addition and/or substitution reactions of $(OC)_{3,2}Fe^{\bullet-}$ with the unsaturated neutrals in this study.

The above data and interpretations lead to the conclusion that, *under the flow conditions of these FA experiments, we are dealing with the electronic ground states of the fragment metal carbonyl negative ions.*

Summary

The reactions of the 16-electron $(OC)_4Mn^-$ and 15-electron $(OC)_3Fe^{\bullet-}$ complexes with propene, 1,3-butadiene, cyclopentadiene, and benzene occur exclusively by η^2 addition of the unsaturated ligand. Allene and acetylene effect competitive substitution and addition. These findings suggest stronger $M{-}L_u$ binding energies for these latter two unsaturated ligands in the product negative ions.

The reactions of $(OC)_4Mn^-$ consistently yield smaller reaction efficiencies compared to the reactions of $(OC)_3Mn^-$ and $(OC)_3Fe^{\bullet-}$ with the same neutral substrate. The rationale for these results is a change in the spin multiplicity from the high-spin triplet ground electronic state of $(OC)_4Mn^-$ (plus singlet L_u) yielding the 18-electron, singlet ground-state product ions $(OC)_4Mn(L_u)^-$. From the isoelectronic relationship between neutral fragment metal carbonyls and the present ions ($Fe(CO)_{5,4,3}$ and $(OC)_{5,4,3}Mn^-$, and $Co(CO)_{4,3,2}$ and $(OC)_{4,3,2}Fe^{\bullet-}$), the ground electronic, states of the ions are assigned to be those of the established ground states for the isoelectronic neutrals.

The reactions of the doubly unsaturated ions $(OC)_3Mn^-$ and $(OC)_2Fe^{\bullet-}$ with propene and benzene formed saturated adduct ions suggested to have the structures $(OC)_xM(H)(\eta^3\text{-}C_3H_5)^-$ and $(OC)_xM(\eta^4\text{-}C_6H_6)^-$, respectively. With 1,3-butadiene as the neutral species, both of these fragment metal carbonyl negative ions form adduct and (adduct − CO) product ions by initial formation of excited η^4-diene intermediates. Collisional quenching competes with unimolecular extrusion of CO from these intermediates. The exclusive formation of the corresponding (adduct − CO) product ions from the reactions of $(OC)_3Mn^-$ and $(OC)_2Fe^{\bullet-}$ with cyclopentadiene is consistent with this same mechanism and stronger binding in the η^4-cyclopentadiene intermediates. The latter product ions were characterized

---

(28) van Koppen, P. A. M.; Brodbelt-Lustig, J.; Bowers, M. T.; Dearden, D. V.; Beauchamp, J. L.; Fisher, E. R.; Armentrout, P. B. *J. Am. Chem. Soc.* **1991**, *113*, 2359.

(29) McDonald, R. N.; Bianchina, E. J. *Organometallics* **1991**, *10*, 1274.

(30) (a) Seder, T. A.; Ouderkirk, A. J.; Weitz, E. *J. Chem. Phys.* **1986**, *85*, 1977. (b) Weitz, E. *J. Phys. Chem.* **1987**, *91*, 3945.

(31) (a) Barton, T. J.; Grinter, R.; Thomson, A. J.; Davies, B.; Poliakoff, M. J. *J. Chem. Soc., Chem. Commun.* **1977**, 841. (b) Poliakoff, M.; Weitz, E. *Acc. Chem. Res.* **1987**, *20*, 408.

(32) Hanlan, L. A.; Huber, H.; Kundig, E. P.; McGarey, B. R.; Ozin, G. A. *J. Am. Chem. Soc.* **1975**, *97*, 7054.

(33) Rayner, D. M.; Nazran, A. S.; Drouin, M.; Hackett, P. A. *J. Phys. Chem.* **1986**, *90*, 2882.

as the $(OC)_xM(H)(\eta^5\text{-c-}C_5H_5)^-$ structures by their failure to undergo further ion/molecule reactions with H_2S, $(CH_3)_3SiH$, and SO_2.

The reactions of $(OC)_3Mn^-$ and $(OC)_2Fe^{\bullet-}$ with acetylene occurred exclusively by ligand substitution terminating in the generation of the ions $M(C_2H_2)_x^-$, where M = Mn, x = 3, and M = Fe, x = 2. These terminal product ions and the intermediate $(OC)Mn(C_2H_2)_2^-$ did not react with D_2, suggesting that they are saturated acetylene complexes rather than metallacycles observed in the cyclooligomerization of acetylene by transition-metal catalysts.

The results observed in the reactions of the fragment negative ions $(OC)_3Mn^-$ and $(OC)_2Fe^{\bullet-}$ with 1,3-butadiene are rationalized by the same mechanism developed for the reaction of the neutral complex $Cr(CO)_3$ with 1,3-pentadiene.

Acknowledgment. We gratefully acknowledge the support of this research by the National Science Foundation.

Synthesis, Characterization, and Reaction Chemistry of Chiral Half-Sandwich Ruthenium Phosphaallyl Complexes

Hong-li Ji,[1a] John H. Nelson,*[,1a] Andre DeCian,[1b] Jean Fischer,[1b] Ljiljana Solujić,[1c] and Emil B. Milosavljević[1c]

Department of Chemistry, University of Nevada, Reno, Nevada 89557, Laboratoire de Cristallochimie et de Chimie Structurale (URA 424-du CNRS), Université Louis Pasteur, 67070 Strasbourg Cedex, France, and Faculty of Sciences, University of Belgrade, 11001 Belgrade, Yugoslavia

Received July 22, 1991

The complexes $[(\eta^5\text{-}C_5H_5)Ru(R_3P)_2(NCCH_3)]^+PF_6^-$, where R_3P is vinyldiphenylphosphine (DPVP) and divinylphenylphosphine (DVPP), reversibly dissociate CH_3CN to form η^3-phosphaallyl complexes. These complexes have been characterized by elemental analyses, infrared spectroscopy, thermal analysis, cyclic voltammetry, and ^1H, $^1H\{^{31}P\}$, $^{13}C\{^1H\}$, $^{31}P\{^1H\}$, $^1H/^{13}C$ HETCOR, 2D-HOJ, NOESY, and COSY nuclear magnetic resonance spectroscopy. Solution equilibrium thermodynamics show that the η^1–η^3 conversion is endothermic and is entropy driven. $[(\eta^5\text{-}C_5H_5)Ru(\eta^1\text{-}Ph_2PCH{=}CH_2)(\eta^3\text{-}Ph_2PCH{=}CH_2)]PF_6$ (**3**) has been characterized by X-ray crystallography. It crystallizes in the monoclinic space group $P2_1/c$ with a = 9.754 (3) Å, b = 22.528 (6) Å, c = 19.840 (5) Å, β = 100.46 (2)°, and Z = 4. The structure was refined by least-squares methods with R_F = 0.035 for 3925 independent observed ($I \geq 3\sigma(I)$) reflections. The Ru–P bond distance for the η^3-$Ph_2PCH{=}CH_2$ ligand (2.276 (1) Å) is significantly shorter than that for the η^1-$Ph_2PCH{=}CH_2$ ligand (2.315 (1) Å). The Ru–C distance to the α-carbon of the η^3-bound phosphine (2.176 (3) Å) is significantly shorter than that to the β-carbon (2.244 (4) Å), and these distances are respectively shorter and longer than the average Ru–C distance to the η^5-C_5H_5 ring (2.215 (4) Å). The C_α–C_β distance (1.399 (5) Å) is considerably longer and the $PC_\alpha C_\beta$ bond angle (119.0 (3)°) considerably smaller for the η^3-phosphine than for the η^1-phosphine (1.306 (5) Å, 127.5 (3)°). Compound **3** reacts with good donor ligands L (L = N_3^-, CH_3CN, $H_2NCH_2CH{=}CH_2$, $(CH_3)_2CHCN$, PhCN, PhNC, and CO) to displace the coordinated vinyl moiety, forming $[(\eta^5\text{-}C_5H_5)Ru(Ph_2PCH{=}CH_2)_2N_3]$ or $[(\eta^5\text{-}C_5H_5)Ru(Ph_2PCH{=}CH_2)_2L]PF_6$. $[(\eta^5\text{-}C_5H_5)Ru(Ph_2PCH{=}CH_2)_2CO]PF_6$ (**11**) has been characterized by X-ray crystallography. It crystallizes in the triclinic $P\bar{1}$ space group with a = 19.065 (4) Å, b = 10.825 (2) Å, c = 9.433 (2) Å, α = 100.08 (2)°, β = 103.37 (2)°, γ = 84.27 (2)°, and Z = 2. The structure was refined by least-squares methods with R_F = 0.054 for 5045 independent observed ($I \geq 3\sigma(I)$) reflections. The two Ru–P bond distances are equal (2.320 (1), 2.324 (1) Å) and longer than those in compound **3**. The $PC_\alpha C_\beta$ bond angles are equal (125.4 (4), 125.5 (5)°), as are the C_α–C_β distances (1.313 (7), 1.316 (8) Å). Reaction of compound **3** with RLi (R = CH_3, CH_3, PhC≡C, $CH_3C{\equiv}C$) induces a novel migration of vinyl from phosphorus to ruthenium, probably by way of λ^5-phosphoranide intermediates.

Introduction

The allyl ligand is prominent[2] in organometallic chemistry. Equilibria between η^1- and η^3-allyls have received considerable attention[3] and are likely to be responsible for the wide range of reactivities exhibited by metal–allyl complexes. Phosphaallyl complexes have only recently been reported[4-9] and were previously expected to be unstable. The syn–anti isomerization[6,10] of phosphaallyl complexes is believed to proceed via η^1–η^3 interconversion of the phosphaallyl in accord with the common mechanism

---

[1] (a) University of Nevada. (b) Université Louis Pasteur. (c) University of Belgrade.

[2] Collman, J. P.; Hegedus, L. S.; Norton, J. R.; Finke, R. G. *Principles and Applications of Organotransition Metal Chemistry*; University Science Books: Mill Valley, CA, 1987; pp 175–182. Clarke, H. L. *J. Organomet. Chem.* **1974**, *80*, 155.

[3] Vrieze, K. In *Dynamic Nuclear Magnetic Resonance Spectroscopy*; Jackman, L. M., Cotton, F. A., Eds.; Academic Press: New York, 1975; pp 441–487.

[4] (a) Appel, R.; Schuhn, W.; Knoch, F. *Angew. Chem., Int. Ed. Engl.* **1985**, *24*, 420. (b) Mathey, F. *J. Organomet. Chem.* **1990**, *400*, 149. (c) Nixon, J. F. *Chem. Rev.* **1988**, *88*, 1353.

[5] Mercier, F.; Fischer, J.; Mathey, F. *Angew. Chem., Int. Ed. Engl.* **1986**, *25*, 357.

[6] Mercier, F.; Hugel-Le Goff, C.; Mathey, F. *Organometallics* **1988**, *7*, 955.

[7] Niecke, E.; Kramer, B.; Nieger, M. *Organometallics* **1991**, *10*, 10.

[8] Mercier, F.; Hugel-Le Goff, C.; Ricard, L.; Mathey, F. *J. Organomet. Chem.* **1990**, *389*, 389.

[9] Hugel-Le, Goff, C.; Mercier, F.; Ricard, L.; Mathey, F. *J. Organomet. Chem.* **1989**, *363*, 325.

[10] Mercier, F.; Mathey, F. *Organometallics* **1990**, *9*, 863.

0276-7333/92/2311-0401$03.00/0